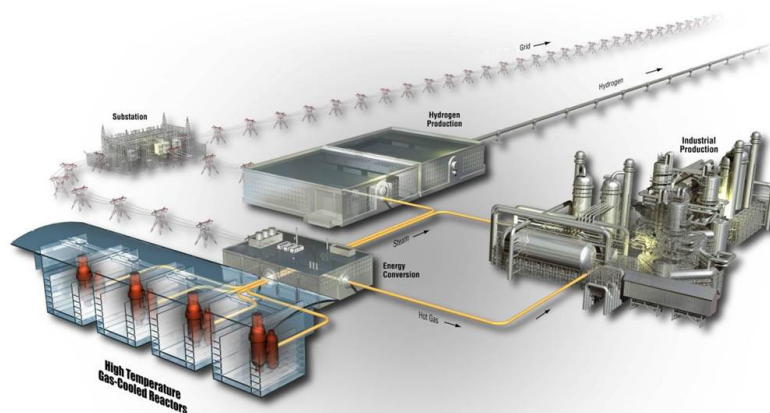




AGC-4 Disassembly Report

August 2023

Philip L. Winston
Idaho National Laboratory



*INL is a U.S. Department of Energy National Laboratory
operated by Battelle Energy Alliance, LLC*

DISCLAIMER

This information was prepared as an account of work sponsored by an agency of the U.S. Government. Neither the U.S. Government nor any agency thereof, nor any of their employees, makes any warranty, expressed or implied, or assumes any legal liability or responsibility for the accuracy, completeness, or usefulness, of any information, apparatus, product, or process disclosed, or represents that its use would not infringe privately owned rights. References herein to any specific commercial product, process, or service by trade name, trade mark, manufacturer, or otherwise, does not necessarily constitute or imply its endorsement, recommendation, or favoring by the U.S. Government or any agency thereof. The views and opinions of authors expressed herein do not necessarily state or reflect those of the U.S. Government or any agency thereof.

AGC-4 Disassembly Report

Philip L. Winston
Idaho National Laboratory

August 2023

Idaho National Laboratory
Advanced Reactor Technologies
Idaho Falls, Idaho 83415

<http://www.ART.INL.gov>

Prepared for the
U.S. Department of Energy
Office of Nuclear Energy
Under DOE Idaho Operations Office
Contract DE-AC07-05ID14517

Page intentionally left blank

INL ART Program
AGC-4 Disassembly Report

INL/EXT-21-63591
Revision 1

August 2023

Technical Reviewer: (Confirmation of mathematical accuracy, correctness of data, and appropriateness of assumptions.)

W. E. Winder

8/16/2023

William E. Winder
ART Graphite R&D Technical Lead

Date

Approved by:

M. Davenport

8/16/2023

Michael E. Davenport
ART Project Manager

Date

Travis R. Mitchell

8/15/2023

Travis R. Mitchell
ART Program Manager

Date

Michelle T. Sharp

8/15/2023

Michelle T. Sharp
INL Quality Assurance

Date

Page intentionally left blank

ABSTRACT

The Advanced Reactor Technologies Graphite Research and Development program is currently measuring irradiated material property changes in several grades of nuclear graphite to predict behavior and operating performance within the core of new high-temperature reactor designs. The Advanced Graphite Creep (AGC) experiment series, consisting of six irradiation capsules, will generate the irradiated graphite performance data for high-temperature gas-cooled reactor operating conditions. All six capsules will be irradiated in the Idaho National Laboratory Advanced Test Reactor (ATR), disassembled in the Hot Fuel Examination Facility (HFEF), and examined at the Idaho National Laboratory Research Center. This disassembly report describes the disassembly and initial evaluation of the graphite specimens contained within the AGC-4 irradiation test capsule (the fourth irradiation capsule of the series).

AGC-4 was irradiated in the ATR East Flux Trap (EFT) during Cycles 157D, 158A, 162A, 162B, 164A, 164B, 166A, and 166B. Approximately 8 displacements per atom (maximum) were achieved. Desired experiment temperatures were exceeded by at least 100°C during the second cycle of irradiation due to the increased flux produced by insertion of the KiJang Research Reactor experiment in the same reactor lobe as the EFT. The capsule was removed from the ATR and transferred to HFEF on May 15, 2020, and unloaded into the HFEF Decon Cell through Penetration 2D on February 26, 2021. It was moved to the HFEF Main Cell Window 3M for disassembly on March 15, 2021. Disassembly and specimen extraction began March 18, 2021, and packaging of the graphite specimens was completed on April 16, 2021. Several anomalies were noted, specifically that the radiological dose rates were nominally an order of magnitude higher than the previous AGC experiments. Due to the high activity of the samples, they were not shipped to the Idaho National Laboratory Research Center (IRC) Carbon Characterization Laboratory, which is only designed for low-activity samples. Additional radiological and mass characterization is being done and was performed at the Materials and Fuels Complex (MFC) Analytical Laboratory to determine the origin of the high activity. After completing this additional characterization to a satisfactory degree, it was possible to transfer a majority of the samples to the Carbon Characterization Laboratory (CCL) to complete the material properties analysis. This report summarizes the disassembly of the AGC-4 experiment and the subsequent survey and segregation of samples found to be in excess of the handling limits of the CCL.

The purpose of this revision (Revision 1) is to discuss the process and results of survey, separation and characterization performed to identify anomalous samples and determine potential sources of high activity. Not all characterization actions have been completed at the time of this revision.

Following the determination that all the individual sample transfer tubes were greater than the nominal upper limit of 100 mR/hr at contact, individual samples were removed from selected tubes to determine whether all samples were high activity. The selected samples were taken from the highest dose rate tubes and found to be in the 1-5 mR/hr range. Based on that knowledge, a decision was made to move the samples from the HFEF decon cell to the MFC Analytical Laboratory Special Projects Glovebox (SPGB) for survey in a low-background location. Removal of the sample tubes from the HFEF Decon Cell for transfer was not completed until November 2021.

Proximity of the SPGB to the MFC-752 Hot Cells allowed for high-activity samples to be transferred into a location where anomalous dose contribution could be characterized by gamma ray spectrometry. The west section of the glovebox was not in use at the time, and thus was available for use for this task. Preparation for that process was made by performing a thorough decontamination of the glovebox to minimize the potential for contaminating otherwise clean samples. Lead brick shielding was installed in the glovebox following engineering evaluation of the load capacity of the glovebox floor. A miniature digital microscope was inserted into the box to allow clear identification of sample numbers without personnel moving the sample unnecessarily close to the window. A medium range ion chamber was set up to provide a means to identify localized high activity within the sample transfer tubes. This sensor was mounted in a steel shield to minimize background from other material within the glovebox or in the

sample tubes. Due to staffing limitations at the Analytical Laboratory, only approximately one-third of the sample tubes were able to be surveyed and samples segregated and decontaminated to the nominal levels that are necessary for work on the benchtop in the CCL. In the interest of completing the survey and segregation task, the remaining sample tubes in the shielded transfer drum were transferred to the Electron Microscopy Laboratory (EML), MFC-774, where personnel were available to complete the survey, decontamination, and repackaging process.

As a general statement, approximately 90% of the samples were determined to be within the range of 1 to 100 mR/hr beta-gamma on contact, and only negligible alpha contamination was detected. The high-activity samples ranged from 100 mR/hr to 8.8 R/hr beta-gamma at contact. Gamma spectrometry of select examples of the high-activity samples indicated that the predominate gamma ray emitting isotope was cobalt-60. Secondary analysis was performed to determine if other contaminants were present. Laser-induced breakdown spectrometry/time-of-flight mass spectrometry measurements indicated the presence of copper as well as nickel and chromium. One sample was also analyzed using X-ray fluorescence, which detected the presence of copper. Conventional mass spectrometry was used to measure metals in solutions that were derived from dissolving the ash residue from oxidizing the samples in an air environment furnace at 750°C. Those analyses also indicated the potential presence of iron and nickel. Isobars at mass 55 and 63 limit the possibility of making a definitive measurement regarding the specific isotope. That sample will be reanalyzed using optical emission spectrometry to do an elemental rather than mass measurement.

ACKNOWLEDGEMENT

Significant time and effort was expended by BJ Camphouse, Lori Muntean, Tony Jones, Cory Kynaston, Julie Heil, Molly Ballinger, Katya Ryan, Tim Higginson, Jose Gonzalez, and Randy Ramirez at MFC Analytical Laboratory, and Andrew Cox, James Newman, Kingston Anderson, Quentin Harris, and Lindsay Stecklein at EML to perform surveys, separate samples, decontaminate, measure and repackage for shipment. Their work is greatly appreciated. Thanks also to Pam Wiscaver for coordinating work at AL and Nick Erfurth for independently doing the TOF/LIBS and XRF measurements.

CONTENTS

ABSTRACT.....	iii
ACRONYMS.....	v
1. DESCRIPTION OF AGC EXPERIMENT	1
2. AGC-4 STATUS.....	3
2.1 Pre-irradiation Examination of AGC-4 Samples	4
2.2 Disassembly of AGC-4 Capsule	4
2.2.1 AGC-4 Capsule Disassembly Activities	5
2.2.2 Dose Rate Evaluations	16
3. CONCLUSIONS FROM AGC-4 CAPSULE DISASSEMBLY ACTIVITIES	17
3.1 Handling and Survey of High-Dose Rate Samples	18
3.2 Visual Inspection of AGC-4 Specimens	25
3.3 Characterization of High-Dose Rate Samples.....	26
4. INTERIM CONCLUSIONS	28
5. REFERENCES.....	28
Appendix A.....	29

FIGURES

Figure 1. CCL glovebox used to visually inspect graphite samples, perform initial dimensional measurement, and repackage samples for storage in the irradiated graphite vault located in Lab C-19.....	2
Figure 2. Dimensional measurement and transfer of samples to plastic storage containers	2
Figure 3. Above: AGC-type test train being lifted from the basket with a lifting fixture cap installed. Below: The AGC-4 test train on the HFEF 3M table, lying horizontally, cutting table in the center of table.....	7
Figure 4. The top (cut) end of AGC-type test train.....	8
Figure 5. Specified cut point for bottom end cap cut.....	8
Figure 6. Sliding graphite body out of pressure tube.....	9
Figure 7. Separating graphite body sections prior to TC and gas line removal. Upper section pistons are visible on the right. Piggyback samples are visible in the catch tray.	10
Figure 8. Upper section pistons are visible on the right. Piggyback samples are visible in the catch tray.....	10
Figure 9. Loose piggyback sample identification.	11
Figure 10. Transferring creep samples into the transfer tube.....	12
Figure 11. Milling graphite body to expose center channel.....	13
Figure 12. 240-degree sector of graphite body with exposed center section. Shiny samples are can design used for HOPG.....	13

Figure 13. AGC-4 shipping tubes survey with and without shielding. (Dose rates are in millirem per hour, indicated in the blue box with a * indicating a contact reading, nominally 2 cm from the face of the detector. Values are beta+gamma, reported with a 3x correction factor).....	15
Figure 14. Image of the caliper measuring the graphite body.....	16
Figure 15. Preliminary results precision gamma scanner creep specimens (Hawkins 2021).	17
Figure 16. Steel detector shield with microscope.	19
Figure 17. Survey equipment in glovebox.	20
Figure 18 Opening the Shielded Drum at EML.....	21
Figure 20. Keyence LS7070M optical micrometer.....	24
Figure 21. Visible projected beam from optical micrometer with aluminum standard.	24
Figure 22. Visual inspection example using miniature digital microscope in glovebox.	25
Figure 23. Rotary pedestal for specimen inspection.	25
Figure 24. X-Ray fluorescence detection of elemental contamination in AGC-4 sample.	26
Figure 25. Image of CAN-114 area scanned by TOF/LIBS detector system.	27
Figure 26. TOF/LIBS spectral and visual display of indicated CAN-114 specimen.	27
Figure A-1 Analysis of Oxidized Sample DA4809	29
Figure A-2. General configuration sketch for optical micrometer.....	30
Figure A-3. MFC AL special projects glovebox general layout for sample survey/decon.....	31

TABLES

Table 1. Cycle Number, Effective Full-Power Days (EFPD), and Cumulative Megawatt-days	4
Table 2. Graphite body physical measurements.	16
Table 3. Preliminary gamma spectrometry data; high-dose AGC-4 specimens.	28
Table A-1. Example survey data for select samples handled in AL hood. (Dose rates are in millirem per hour, OW is Open Window, nominal total beta+gamma, CW is Closed Window, nominally gamma only)	30
Table A-2. Interim Listing of Samples in Excess of 100 mR/hr (* indicates partially or completely illegible, or uncertain ID)	31

ACRONYMS

AGC	Advanced Graphite Creep
AL	Analytical Laboratory
ART	Advanced Reactor Technologies
ATR	Advanced Test Reactor
CAN	Can, Alternate Term for Container
CCL	Carbon Characterization Laboratory
DOE	Department of Energy
dpa	Displacements per Atom
DOA	DTCCI Overpack Adapter
DR	Direct Reading
DTCCI	Dry Transfer Cubicle Cask Insert
EFPD	Effective Full- Power Days
EFT	East Flux Trap
EML	Electron Microscopy Laboratory
EMM	Electromechanical manipulators
HDG	High-Dose Graphite
HFEF	Hot Fuel Examination Facility
HOPG	Highly Oriented Pyrolytic Graphite
ID	Inside Diameter
INL	Idaho National Laboratory
IRC	Idaho National Laboratory Research Center
KJRR	KiJang Research Reactor
LIBS	Laser-Induced Breakdown Spectrometry
MCNP	Monte Carlo N-Particle
MFC	Materials and Fuels Complex
NEFT	Northeast Flux Trap
OD	Outside Diameter
ORNL	Oak Ridge National Laboratory
PIE	post-irradiation examination
RT	Room Temperature
SPGB	Special Projects Glovebox
TC	Thermocouple
TOF	Time-of-Flight (Mass Spectrometry)
XRF	X-ray fluorescence

Page intentionally left blank

AGC-4 Disassembly Report

1. DESCRIPTION OF AGC EXPERIMENT

The Advanced Reactor Technologies (ART) Graphite Research and Development program is currently measuring irradiated material properties to predict the behavior and operating performance of new nuclear graphite grades available for use within the cores of new high-temperature reactor designs. The Advanced Graphite Creep (AGC) experiment series, consisting of six irradiation capsules, will generate irradiated graphite performance data for high-temperature gas-cooled reactor operating conditions. The AGC experiment is designed to determine the changes to specific material properties such as thermal diffusivity, thermal expansion, elastic modulus, mechanical strength, irradiation-induced dimensional change rate and irradiation creep for a wide variety of nuclear grade graphite types over a range of temperature and fluence conditions. A series of six capsules containing graphite test specimens will be used to expose graphite test samples to a dose range of 1–7 displacements per atom (dpa) at three different temperatures (600, 900 and 1,200°C) as described in the Graphite Technology Development Plan. Since irradiation-induced creep within graphite components is considered critical to determining the operational life of the graphite core, some of the samples will also be exposed to an applied load to determine the creep rate for each graphite type under both temperature and neutron flux. (Windes 2010)

Irradiation of AGC-1, 2, 3, and 4 has been completed, as has characterization of AGC-1, 2, and 3. The final two capsules in the series are High-Dose Graphite (HDG) experiments (HDG-1 and 2) in which previously irradiated graphite specimens are repackaged into a new capsule for further irradiation. All six AGC-type capsules in the series are to be irradiated in the Advanced Test Reactor (ATR). AGC-1 and AGC-2 were irradiated in the south flux trap and AGC-3 through HDG-2 are to be irradiated in the East Flux Trap (EFT). The change in flux traps was due to program irradiation priorities that required the AGC experiment to be moved to accommodate fuel irradiation experiments. After irradiation, all AGC-type capsules cool in the ATR Canal, are sized for shipment, and shipped to the Materials and Fuels Complex (MFC) where the capsule will be disassembled in the Hot Fuel Examination Facility (HFEF). During disassembly, the metallic capsule is machined open and the interior graphite body containing the samples is removed. Individual creep and piggyback samples are removed from the graphite body and packaged with the intent that they would be loaded into a shielded drum and shipped to the Idaho National Laboratory Research Center (IRC) Carbon Characterization Laboratory (CCL) for post-irradiation examination and storage for any future testing.

The CCL is located in Labs C-19 and C-20 of the IRC. It was specifically designed to support graphite and ceramic composite research and development activities. The CCL is an unshielded laboratory space equipped to characterize low-activity irradiated high-purity graphite, carbon-carbon composites, and silicon-carbide composite materials. Limited-activity irradiated and nonirradiated materials properties are measured working with the samples on the bench top. All test specimens processed through the CCL receiving glovebox undergo visual inspection and dimensional measurement. and are logged for shielded storage in the irradiated graphite vault located in Lab C-19, shown in Figures 1 and 2.



Figure 1. CCL glovebox used to visually inspect graphite samples, perform initial dimensional measurement, and repackage samples for storage in the irradiated graphite vault located in Lab C-19

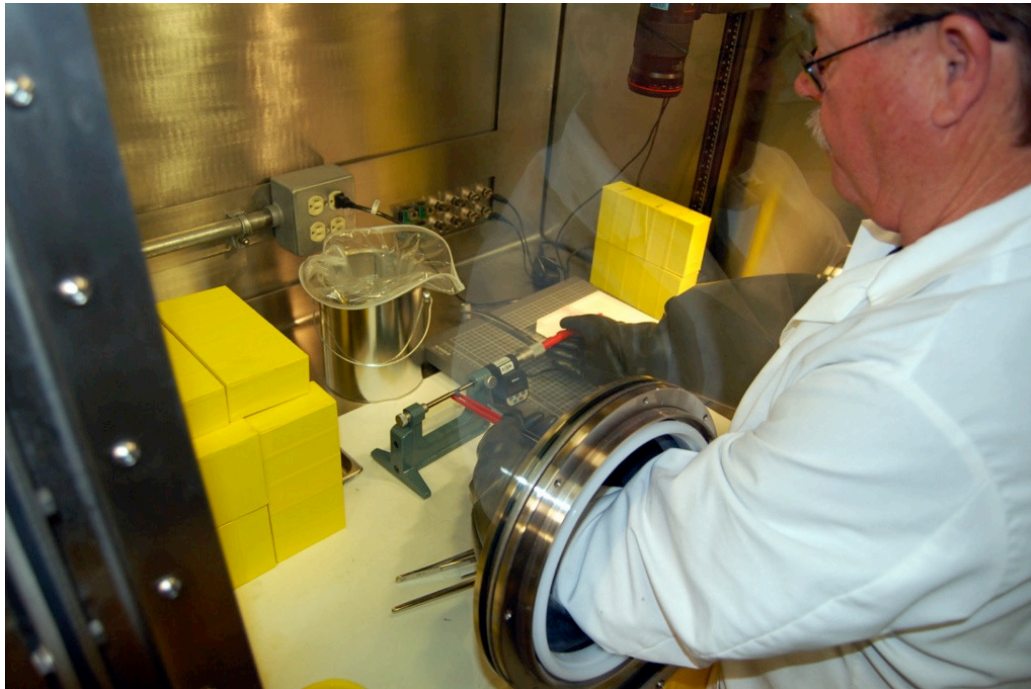


Figure 2. Dimensional measurement and transfer of samples to plastic storage containers

2. AGC-4 STATUS

Activities for AGC-4 began with the pre-irradiation characterization of all graphite samples to be inserted into the AGC-4 capsule. Following characterization, the samples were loaded into the AGC-4 capsule in the summer of 2009. The completed AGC-4 capsule was then inserted into the ATR East Flux Trap. The experiment was irradiated during ATR Cycles 157D, 158A, 162A, 162B, 164A, 164B, 166A, and 166B. ECAR-5345, As-Run Physics Analysis for the AGC-4 Experiment Irradiated in the ATR, derived a cumulative received dose of approximately 8 dpa. The desired experiment average temperatures of 800°C were exceeded by at least 100°C during the second cycle of irradiation. It is presumed that the temperature excursion was due to unexpectedly high flux resulting from the insertion of the KiJang Research Reactor (KJRR) experiment in the Northeast Flux Trap during the same irradiation cycle as AGC-4. After irradiation was completed, the capsule was removed from the ATR and transferred to the MFC HFEF on May 15, 2020. The experiment was unloaded from the shipping cask into the HFEF Decon Cell through Penetration 2D on February 26, 2021. It was moved to the HFEF Main Cell Window 3M for disassembly on March 15, 2021. Disassembly and specimen extraction began March 18, 2021, and packaging of the graphite specimens into transfer tubes to be loaded into the shielded shipping drum was completed April 16, 2021. During preparations for shipping the samples to the INL Carbon Laboratory it was observed that radiological dose rates of the packaged samples exceeded those measured for previous experiments by at least an order of magnitude. This report summarizes the disassembly and packaging of the AGC-4 graphite specimens.

Calculation of heating rates and expected fluence was performed in ECAR-5345, As-Run Physics Analysis for the AGC-4 Experiment Irradiated in the ATR. (Davenport 2021) The following is excerpted from that document:

The AGC-4 as-run specimen neutron fast fluence ($E > 0.1$ MeV), DPA, and material heat rate calculations were performed using a general-purpose Monte Carlo N-Particle (MCNP) code.

Heating Rates:

The average East lobe power across all eight cycles was 20.8 MW, used to scale the average heating results.

In comparing the heating rates of the AGC-4 graphite samples with and without the KJRR experiment inserted, the heating rates across Cycle 158A, with the KiJang Research Reactor experiment (KJRR) inserted within the Northeast Flux Trap (NEFT), were calculated to be approximately 5% higher at core centerline for Stack 2 and Stack 3 (the two graphite stacks closest to the NEFT), tapering off to about 1.5% higher toward the axial ends of the core. The heating rates for Stack 7 (center stack) were calculated to be higher by approximately 4% at core centerline.

Although KJRR increased the heating rates of the graphite samples within the AGC-4 experiment during Cycle 158A with a maximum East lobe power of 23.67MW, the absolute maximum heating occurred during Cycle 162A wherein the East lobe experienced a spike of 24.31MW.

Fluence:

At the end of the eighth cycle, the graphite samples incurred a fluence that ranged between $2.5 \times 10^{21} \frac{n}{cm^2}$ and $2.5 \times 10^{22} \frac{n}{cm^2}$ depending on the location of the sample axially within the EFT of the ATR.

Predicted sample dose in terms of effective full-power days and megawatt-days is shown in Table 1.

Table 1. Cycle Number, Effective Full-Power Days (EFPD), and Cumulative Megawatt-days

Cycle	East Lobe Power [Ave/Max] (MW)	EFPDs	Cumulative EFPDs	MW	MWd	Cumulative MWd
157D-1	21.1 / 22.6	59.7	59.7	21.05	1256.7	1256.7
158A-1	22.1 / 23.1	52.2	111.9	22.12	1154.7	2475.2
162A-1	22.2 / 23.5	62.0	173.9	22.22	1377.6	3864.1
162B-1	18.7 / 20.0	38.5	212.4	18.65	718.0	3961.3
164A-1	20.0 / 21.4	54.9	267.3	20.04	1100.2	5356.7
164B-1	20.0 / 21.8	64.1	331.4	20.03	1283.9	6637.9
166A-1	21.3 / 38.1	62.5	393.9	21.34	1333.8	8405.8
166B-1	21.2 / 22.0	60.0	453.9	21.17	1270.2	9609.1

2.1 Pre-irradiation Examination of AGC-4 Samples

A complete pre-irradiation testing and characterization program was conducted in 2012 on all graphite samples inserted into AGC-4 capsule. The properties measured were bulk density and electrical resistivity as well as elastic constants including dynamic Young's modulus (fundamental frequency method), sonic elastic constants including Young's modulus, shear modulus, and Poisson's ratio; ambient temperature thermal conductivity and thermal expansion (from room temperature [RT] to 800°C). (Swank 2012)

2.2 Disassembly of AGC-4 Capsule

After irradiation was completed, the AGC-4 capsule was stored in the ATR Canal to allow the activity of the steel pressure tube section of the capsule to decay to acceptable shipping levels. After radiological cooling, the ends of the pressure boundary were cut off to remove the upper pneumatic ram compressive loading components and the lower pressure tube, including the stack stirring pneumatic bellows. The sectioning was performed using a remotely operated band saw in the ATR Dry Transfer Cubicle (DTC). Once the AGC-4 test train was sectioned to remove the mechanical loading components (i.e., top pneumatic ram and bottom bellow sections) the steel pressure boundary section with irradiated graphite specimens was loaded into the Dry Transfer Cubicle Cask Insert (DTCCI). The DTCCI is a shielded package, which was designed to contain dry experiments while they are moved inside ATR from the DTC to a shipping container for transport to another facility. The DTCCI was designed to fit into the GE-2000 cask which would provide additional shielding and structure for over-the-road transport. Due to cost and availability issues, the GE-2000 was replaced by the DTCCI Overpack Adapter (DOA), which is a shielded package that was designed and fabricated specifically by the ART program for onsite INL shipments. This transfer package was designed to simplify loading and handling of the DTCCI and optimize mating to the HFEF cells for experiment movement into the cell. The AGC-4 graphite test train was the first irradiated experiment shipped from ATR to MFC using the DOA system.

Unfortunately, the rescue hoist within the HFEF Main Cell failed in October 2020. This is the primary hoist used to replace electromechanical manipulators (EMM) and crane components in the HFEF Main Cell. The hoist was engaged on an EMM carriage when the motor brake failed to engage the load. Because the HFEF Main Cell operations are highly interdependent, only limited in-cell activities could be performed and severely restricted AGC-4 disassembly activities. EMMs are required to move components to the operating windows, and when one of the two in-cell is out of service, the other is typically reserved to supplement repair functions. Hence, the AGC-4 experiment and disassembly equipment could not be moved to an operating window until the hoist was repaired. Due to the complexity of performing the repair, the hoist was not declared operational until February 2021. Disassembly activity was initiated mid-March 2021.

The interior of the AGC-4 capsule was constructed of two graphite body sections approximately 2 inches in diameter by 20 inches long (for a total length of approximately 49 inches before irradiation), held together by bayonet joints. Seven channels were bored axially down the length of the graphite body: one central channel and six on the outer radius surrounding the central channel. Graphite samples in the six radial channels of the upper half of the graphite body were compressively stressed while the graphite samples in the lower half were left unloaded as control samples. The samples in the central channel, upper and lower halves, were unstressed. Twenty-six spacer samples containing flux wires were located in upper, middle, and lower positions within the six radial channels to ascertain the accumulated dose in the samples throughout the capsule. The top and bottom halves were separated at the graphite body centerline and pistons between each half transmit the pneumatic force from the stack stirring pneumatic bellows to allow the test samples in each stack to be stirred during reactor shutdown and outages. A center channel running the entire length of the graphite body contained unstressed piggyback samples that consisted of a multiplicity of small thermal test buttons of the five main graphite grades, experimental graphite grades, and Highly Oriented Pyrolytic Graphite (HOPG) specimens. Details of the generic AGC capsule are shown on INL Drawing 630430. Specifics of the AGC-4 design are shown in INL Drawings 604551 through 604555. Specifics of the assembly and irradiation of AGC-4 are found in the data package DP-AGC-4. (Davenport 2019)

Difficulties were encountered during sample pushout for all stacks (radial and center stacks). All samples from the outer perimeter stacks were eventually pushed out but required significantly higher force than previously experienced the disassembly of past AGC test trains. Pushout of center stack samples was not successful (the maximum designed pushing force of 75 pounds was exceeded). Alternatives for pushout were considered, but it was concluded that the least destructive approach was to mill through the graphite body to release the samples in the center channel. All flux wire samples were recovered and are to be transferred to another facility for gamma counting following initial investigation of the excessive dose rates that have been observed within the graphite samples. The graphite body debris will be discarded.

2.2.1 AGC-4 Capsule Disassembly Activities

Due to the high-radiation levels from the steel pressure tube and other metal components of the test train, the AGC-4 test train capsule was disassembled in the HFEF main hot cell. A summary of the AGC-4 disassembly highlights is presented in this section.

The general AGC-4 disassembly task sequence was planned as follows:

1. Remove the graphite body containing the samples from the steel pressure boundary tube.
2. Remove the gas lines that provided helium and neon gas flow for temperature control and actuate the stack stirring bellows.
3. Remove the accessible thermocouples that penetrate each elevation in the graphite body.

4. Separate the two graphite body sections and push out the 0.25-inch-thick piggyback samples from the center position of the graphite body.
5. Push the individual radial position creep samples into a sorting station for visual identification by sample number.
6. Separate the spacers containing the flux wires from the test specimens for individual analysis.
7. Insert all graphite specimens into a Lexan tube to protect the samples from contamination in the HFEF Main Cell and prevent damage during transport to the CCL.
8. Perform physical measurement of the graphite body. Measure the length of each graphite body section length.

AGC-4 disassembly began March 17, 2021, when the test train capsule was removed from its shipping basket and moved to the disassembly table at HFEF Main Cell Window 3M. Visual examination of the exterior of the pressure boundary tube showed no noticeable blemishes or defects.

The test train was clamped in the collet of the pipe cutter attachment to remove the outer steel pressure tube. Based upon lessons learned from AGC-2 disassembly, seen in Figure 3, the cutter was attached to make a cut approximately 1-3/8 inches above (to the right in the image) the steel bottom cap. The cap remained connected to the thermocouples and gas lines and the heat shield was intact. Operators encountered interference in inserting the test train into the cutter collet due to tighter than expected tolerances in the newly acquired 2.5-inch inside diameter (ID) collet. As a workaround, a 2.75-inch collet that was available in the hot cell was fitted with a split-shell spacer to allow more convenient insertion and clamping in the cutter. This approach allowed cutting to proceed, although when the cut reached its final stage, the remaining thin layer of steel tended to catch on the cutter bits, requiring the cutter to be reversed and restarted several times. The cap was eventually separated by severing the remaining thin layer manually. A general view of the cut end of the experiment is shown in Figure 4. Figure 5 shows the nominal cut line location for removing the end cap.

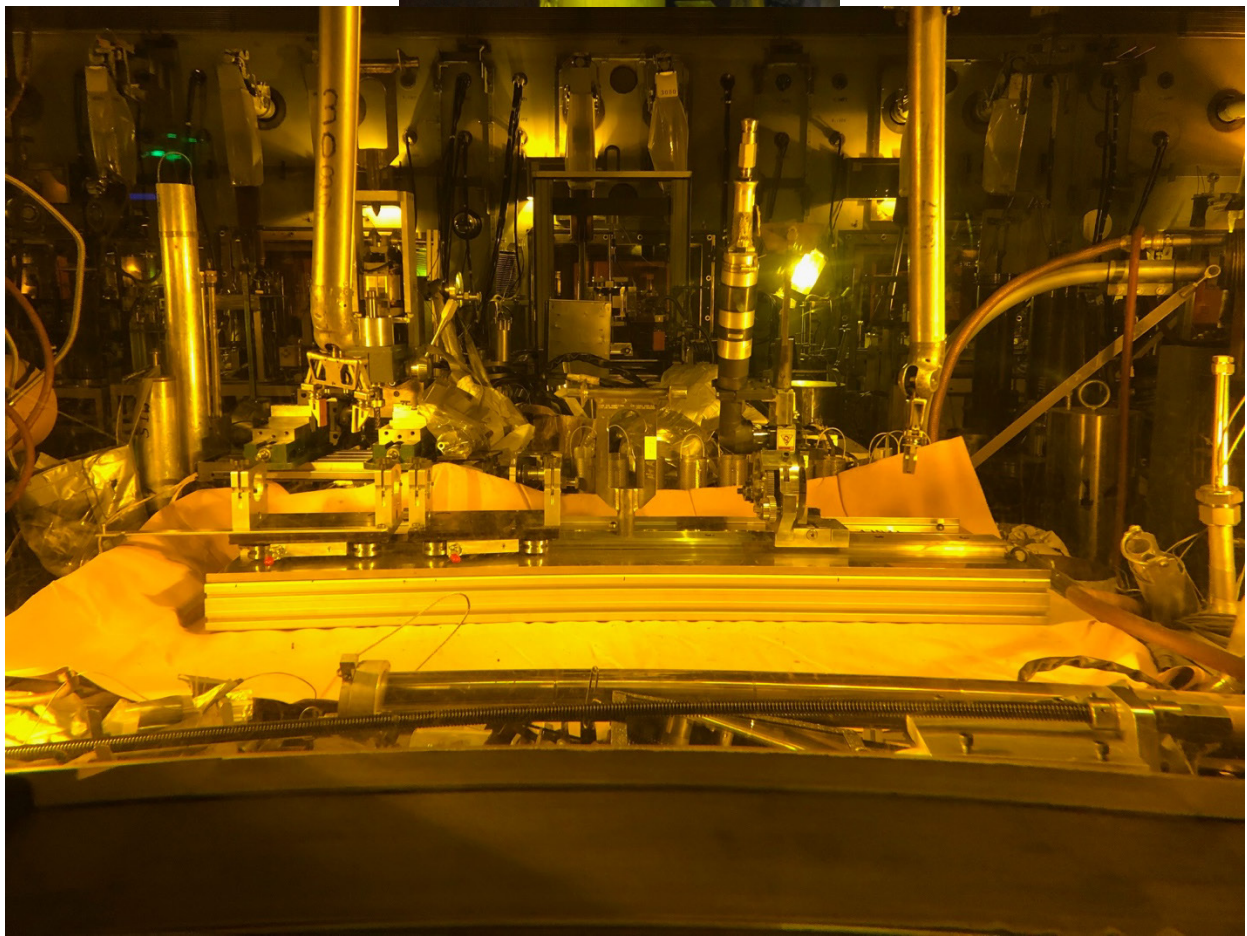
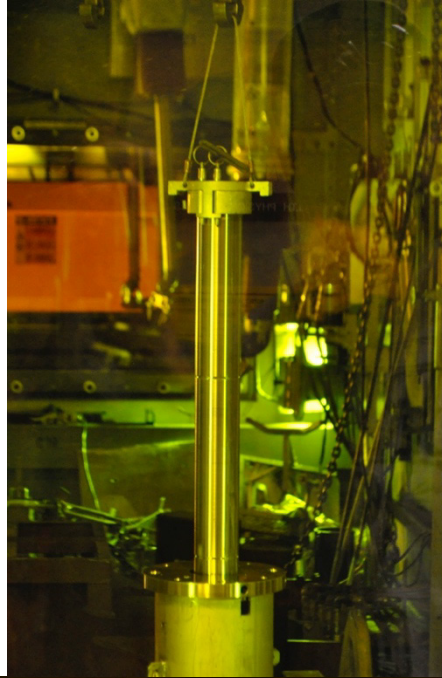


Figure 3. Above: AGC-type test train being lifted from the basket with a lifting fixture cap installed. Below: The AGC-4 test train on the HFEF 3M table, lying horizontally, cutting table in the center of table.

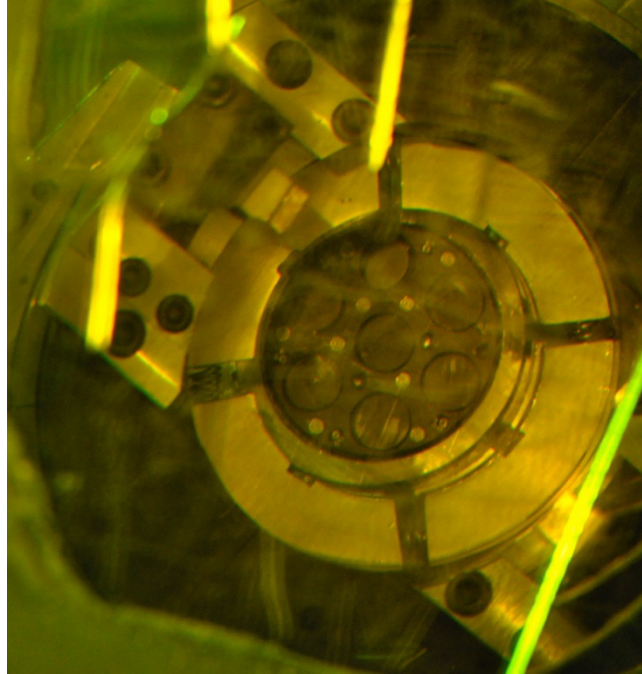


Figure 4. The top (cut) end of AGC-type test train.

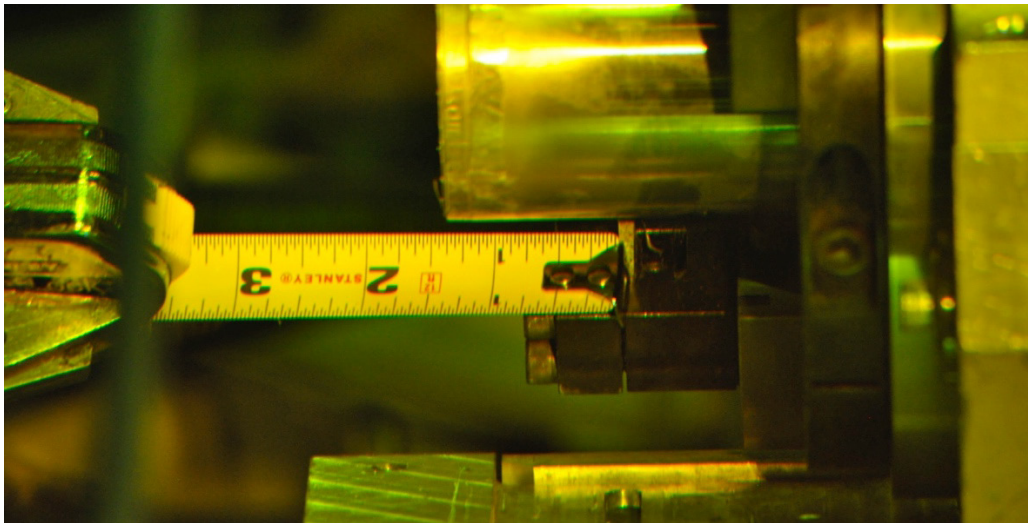


Figure 5. Specified cut point for bottom end cap cut.

The steel pressure tube was removed by sliding the tube laterally off the graphite body, as shown in Figure 6 first manually using the master-slave manipulators, then by reversing the components (flipping end for end) and using the leadscrew drive to pull the tube off in sequential clamping and repositioning of the clamp carriages. (Clamp the tube in the left [stationary] carriage, clamp the end cap in the right [driven] carriage and operate the leadscrew with the pneumatic drive to pull the cap and graphite body out of the steel tube.)

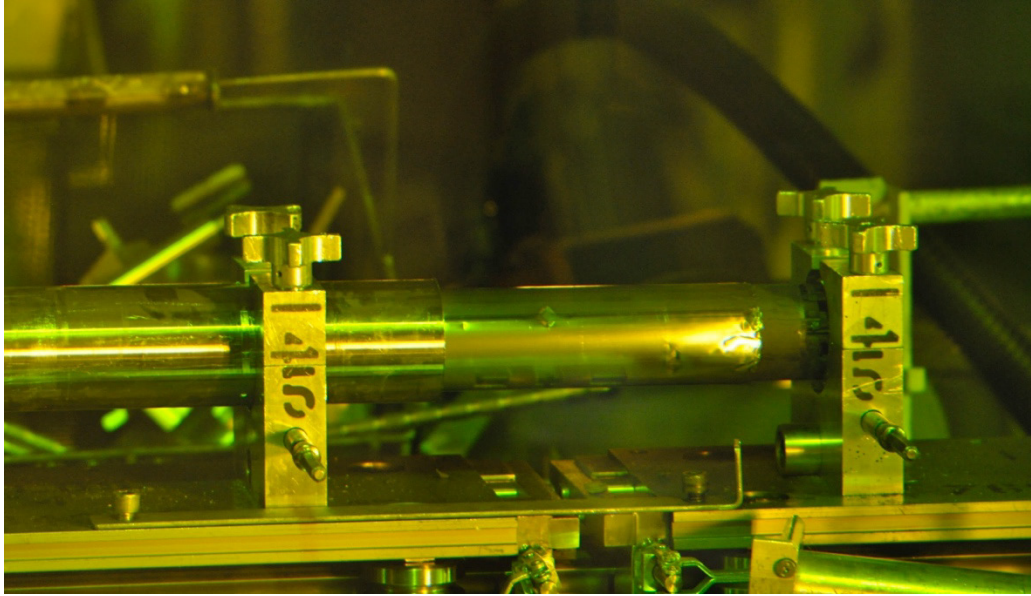


Figure 6. Sliding graphite body out of pressure tube.

To remove the graphite body, the steel tube was mounted in the right carriage, and using the table leadscrew, driven to the left carriage which was locked in position on the rail. The left carriage right clamp had the pushout probe installed, and the graphite body was extruded with minimal drama. Insertion of sequential probe pieces into the pressure tube allowed the graphite body to be pushed out to the point where manual pulling with the manipulator was sufficient to complete removal of the graphite body from the pressure tube. The open end of the pressure tube was capped to prevent loss of samples during the lateral movement. Except for separation at the bottom cap where the cut was made, the steel heat shield remained in place for the entire lateral move of the steel tube. Some dimpling was visible at a section joint in the graphite body.

Once the pressure tube was separated, it was tipped into a catch tray to verify that no loose pieces had fallen into the tube during the removal process.

Because the heat shield was intact, a tweezer tip was slipped under the steel foil to tear the foil. The tear was manipulated until the entire graphite body was exposed.

When the heat shield was removed, it was apparent that the center joint of the graphite body had separated approximately 1/8 inch. The graphite body was placed in the carriage clamps on the cutter table using the 2.5-inch outside diameter (OD) to 2-inch ID spacers. A catch pan was placed under the joint to catch any wayward items. The catch pans used were an updated design that mounted to the test train section carriage clamps.

Due to simplification of the table design, the leadscrew mount did not include an integrated pushout plug for the graphite body. A separate 1.9-inch OD \times 4-inch-long plug was fabricated and mounted in the left carriage clamp.

The graphite body sections were then separated using a variation of the clamping and leadscrew pulling process used for removing the graphite body from the steel pressure tube as illustrated in Figure 7. The samples in the lower section (left side) of the graphite body were free to slide out at the joint and, due to the vibration of the pneumatic drive on the leadscrew, required frequent attention to push back in until the gas lines and thermocouples (TCs) could be removed. Another view of the separation showing the thermocouples and samples is Figure 8.

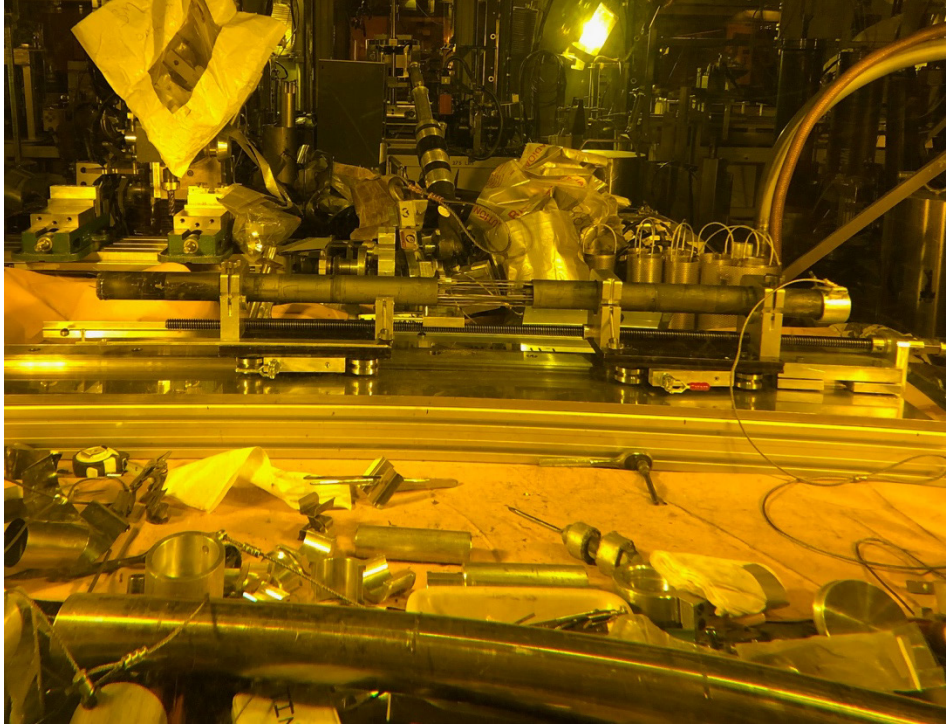


Figure 7. Separating graphite body sections prior to TC and gas line removal. Upper section pistons are visible on the right. Piggyback samples are visible in the catch tray.

The gas lines and thermocouples were accessible following separation and were removed from the graphite body by manually pulling with the master-slave manipulators.

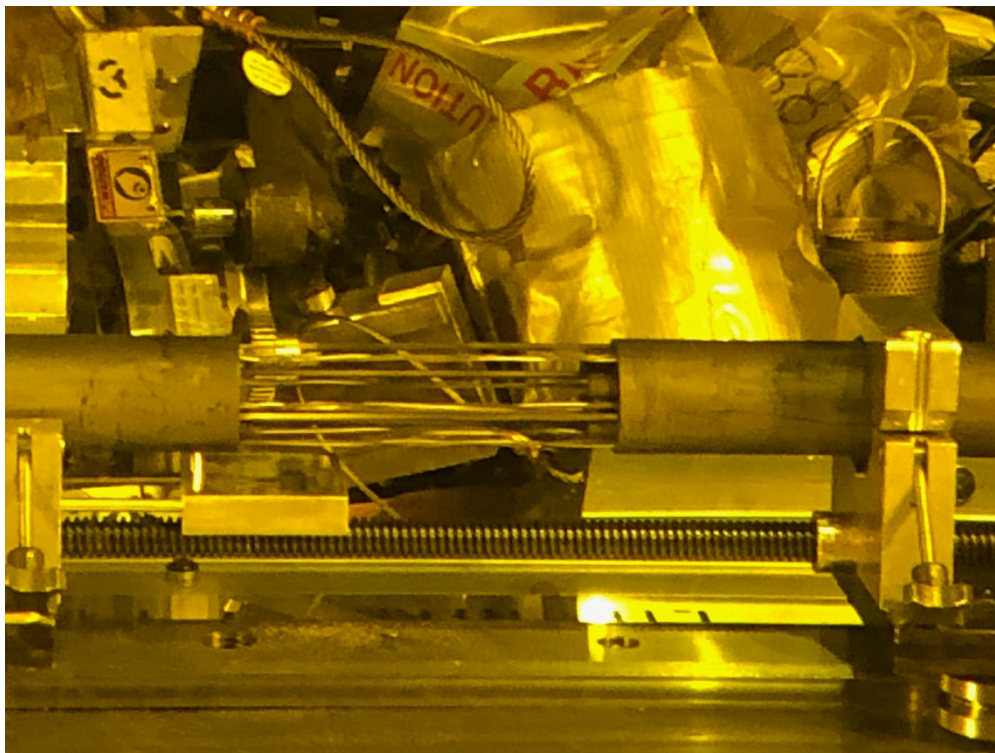


Figure 8. Upper section pistons are visible on the right. Piggyback samples are visible in the catch tray.

The piggyback samples that had fallen out at the center joint were retrieved and identified visually as seen in the example in Figure 9.

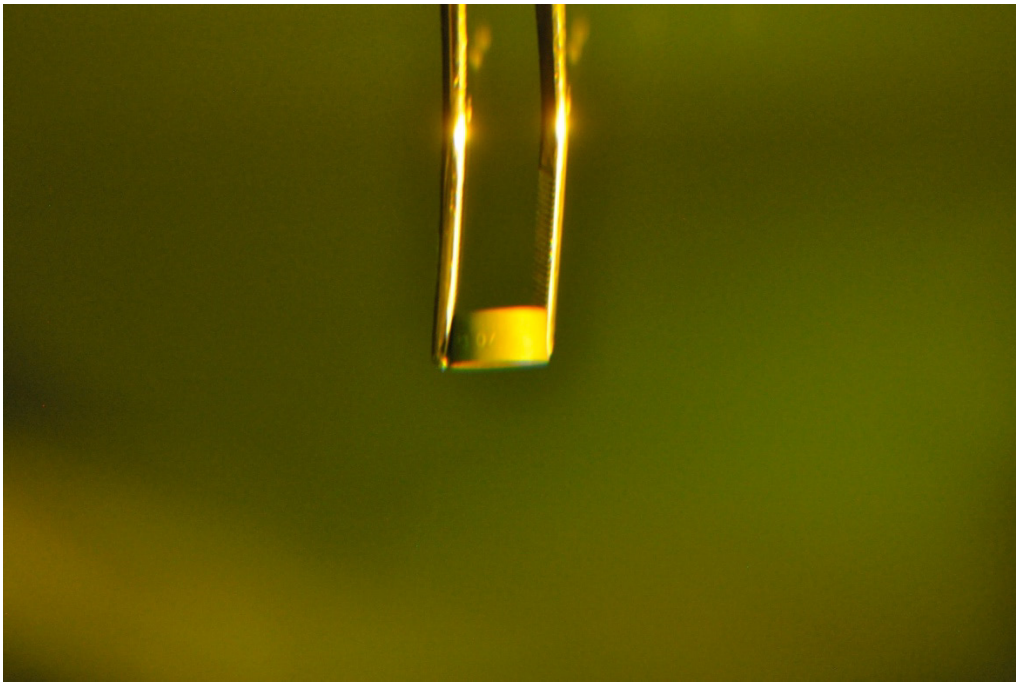


Figure 9. Loose piggyback sample identification.

Once the graphite body sections were removed from the pressure tube, they were individually lifted with the master-slave manipulator and transferred to the radial position insert of the sorting table. Once secured on the sorting table, a receiving tube was mounted onto the receiving end of the sorting table tray to receive specimens pushed out from the graphite body.

Attempts were made to push out the center stack of piggyback samples, but there was no success. Unlike previous experiments in which care was required to prevent piggybacks from falling out, the sorting table force gauge indicated greater than 50 pounds, and no movement was achieved. Efforts were redirected to the radial stacks.

Difficulties were encountered during pushout of radial stacks, as the lower section stacks required greater than 30 pounds force (indicated on the sorting table force gauge) to get the stacks to move. Eventually, the lower stacks were removed, identified, and transferred to the shipping tubes. Attempts to push out the upper section stacks were directed from the left to right with the graphite body section oriented with the previously “up” section to the right. This meant that the stack was being pushed against the shuttle pistons, which were in their partially extended position. Following consultation, it was determined that it should be possible to reverse the graphite body orientation and push against the shuttle pistons to remove the stacks. After repositioning, the pushout was performed successfully, although requiring approximately 60 pounds force to break the stacks loose to allow movement.

As the radial stacks were pushed out, the spacers that contained the flux wires were identified and separated for later fluence capsule recovery as shown in Figure 10. All graphite specimens contained within each uniquely identified transfer tube were identified and listed in the appendix of the operating procedure.

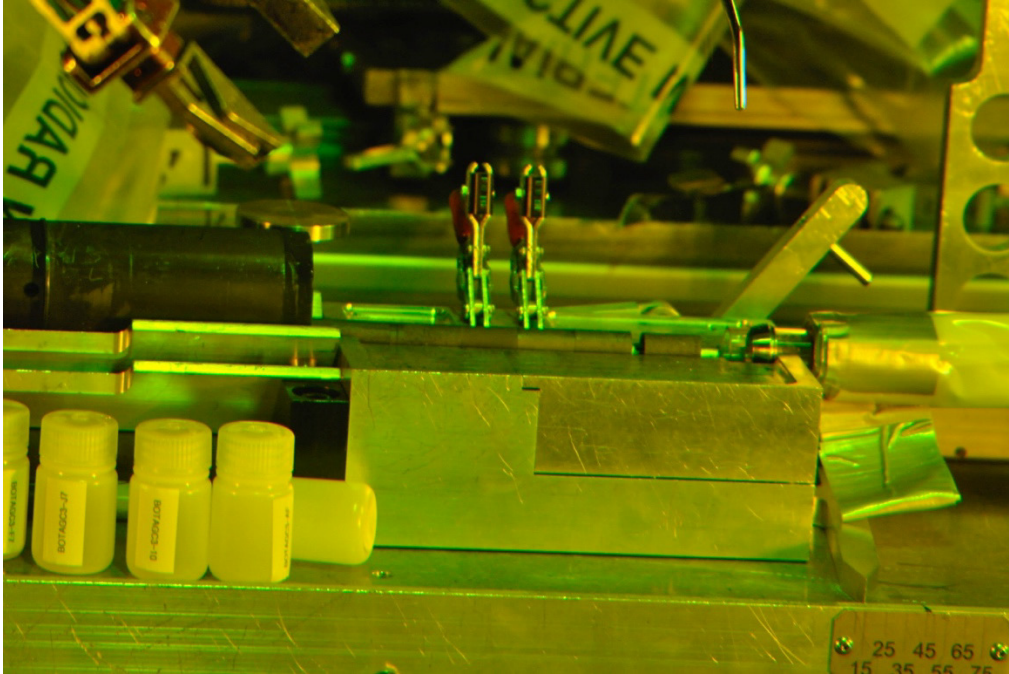


Figure 10. Transferring creep samples into the transfer tube.

Flux wires were removed from the spacers and placed in small cryo-vials for shipping and direct gamma ray counting. All flux wires will be analyzed to verify the accumulated dose calculations.

Following removal of the creep and unstressed radial channel samples, attention was brought to bear upon the center stack samples. Pushing was not successful, exceeding the maximum indicated value of 75 pounds per sorting table. Only six to ten of the piggyback samples were free enough to fall out when the graphite body was raised to the vertical position in either end orientation.

Alternatives for pushout were considered, but it was concluded that the least destructive approach was to mill through the graphite body to release the samples in the center channel. The HFEF Main Cell has a modified, remotely operable Wabeco F1210 milling machine with digital position readout that is stationed on the 3M table. The unit has lateral travel of 20 inches and front to back movement of 6 inches. It was developed for fabricating tensile and bend test samples of irradiated cladding. The unit has a suction unit that can collect fines to prevent the spread of contamination. Figure 11 shows the mill in operation. Because it was located at the same window where AGC-4 was being disassembled, it was concluded that the 3/8-inch OD mill bits that are primarily used on the machine could be used to mill a slot over the length of the graphite body sections to allow access to the center stack. Two slots were machined in line with radial channels that were 120 degrees apart. Two passes were used to get to near the center channel wall depth. Milling depth was controlled to no closer than 0.030 inches to assure that the samples were not contacted by the mill bit.

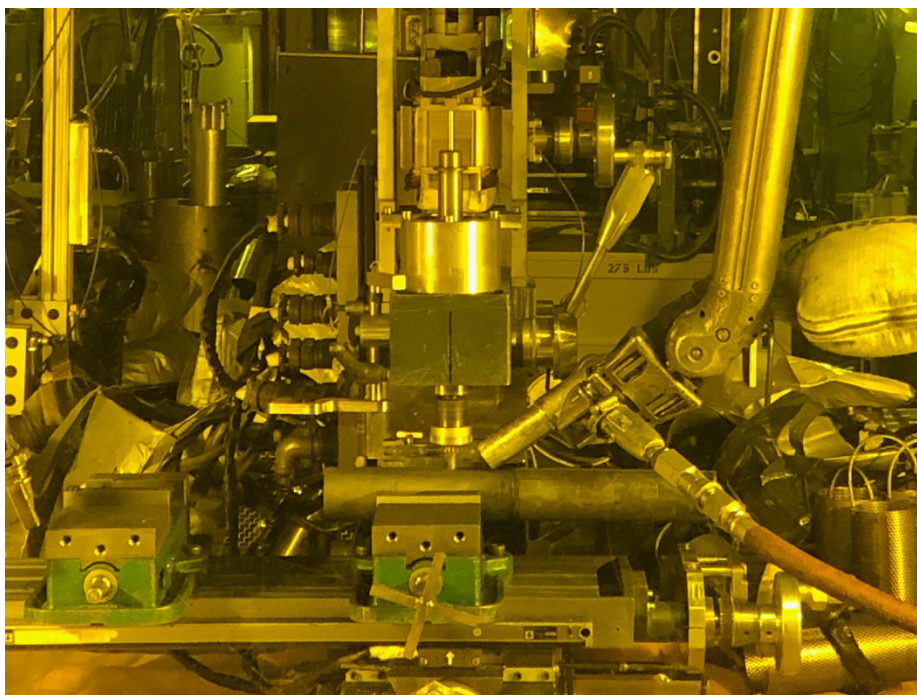


Figure 11. Milling graphite body to expose center channel.

After the two slots had been completed, the 120-degree sector was broken out of the graphite body section by prying with a small screwdriver. The exposed samples were generally intact and were moved out of the channel manually by using a tweezer. The piggyback samples appeared to be restricted from movement by the type of can used for HOPG samples (see Figure 12).



Figure 12. 240-degree sector of graphite body with exposed center section. Shiny samples are can design used for HOPG.

In the lower section, the graphite body broke across its diameter into two pieces while removing the steel gas control rings from the section. The two pieces were machined separately, and the 120-degree sectors were removed with minimal effort. Once exposed, some fairly gnarled-looking samples were observed, but most were generally intact, with visible identification numbers. In the lower piece of the lower section, one recalcitrant graphite can was not removable with tweezers. The can was eventually recovered after the other samples were removed.

An attempt was made to machine the 26-inch-long upper section as a single piece, which required lateral reclamping to achieve the full traverse. At least one thermocouple was encountered by the mill during the cut. During the second of the long cuts, the graphite body section separated at the slot for the gas control ring, leaving the 120-degree sector intact while severing the 240-degree lower piece.

Once opened, the sectors revealed at least two stuck graphite cans in the longer of the two sections, but all were removable when tweezer effort was applied. Some surfaces were damaged to the extent that only partial identification was possible.

Despite indications that the HOPG sample containers (cans) caused interference during specimen pushout, the cans remained closed due to the screw-top container design. AGC-1 and -2 used a slip-fit lid that tended to separate during sample removal, allowing the HOPG specimen to fall out.

To minimize potential for contamination from the HFEF Main Cell, each transfer tube was covered with three layers of polyethylene sleeving, allowing a layer to be removed as the tubes are moved from different contamination zones. One layer is removed when transferred from the main cell to the decon cell, one is removed for transfer from decon cell to the Hot Repair Area, and one is removed when the tube is transferred into a new heat-sealed sleeve as it is transferred out of the Hot Repair Area and placed in the shielded shipping drum.

The radiation levels of all transport tubes containing the graphite test specimens were surveyed at the sample station at decon cell Window 4D prior to movement to the Hot Repair Area. The maximum individual tube dose rate was reported as 3000 mR/hr. The lowest individual tube value was approximately 1000 mR/hr. The minimum values are approximately ten times that seen for AGC-1, 2, or 3.

First impressions suggested that the transfer tubes might be contaminated due to exposure to conditions in the HFEF Main Cell. The transfer tubes were decontaminated using window cleaner in the decon cell, and all the survey smears counted as clean. The dose rates were measured using a Ludlum Model 7 ion chamber with a mid-range 0 to 20,000 mR/hr detector. To determine potential for using shielding to individual tubes were also surveyed with a 1/2-inch-thick steel plate and a 1/2-inch acrylic plate between the source and the detector. This test indicated only that the steel-acrylic combination only reduced the indicated dose rate at most by a factor of four, as shown in Figure 13. The contact value is shown in the blue box with DR in the upper section. The values shown have been corrected by the Survey Report program by multiplying the raw instrument reading by three for conservatism. Note that none of the surveys made in the decon cell can be considered to be quantitative because the nominal background dose is approximately 500 mR/hr in the cell.

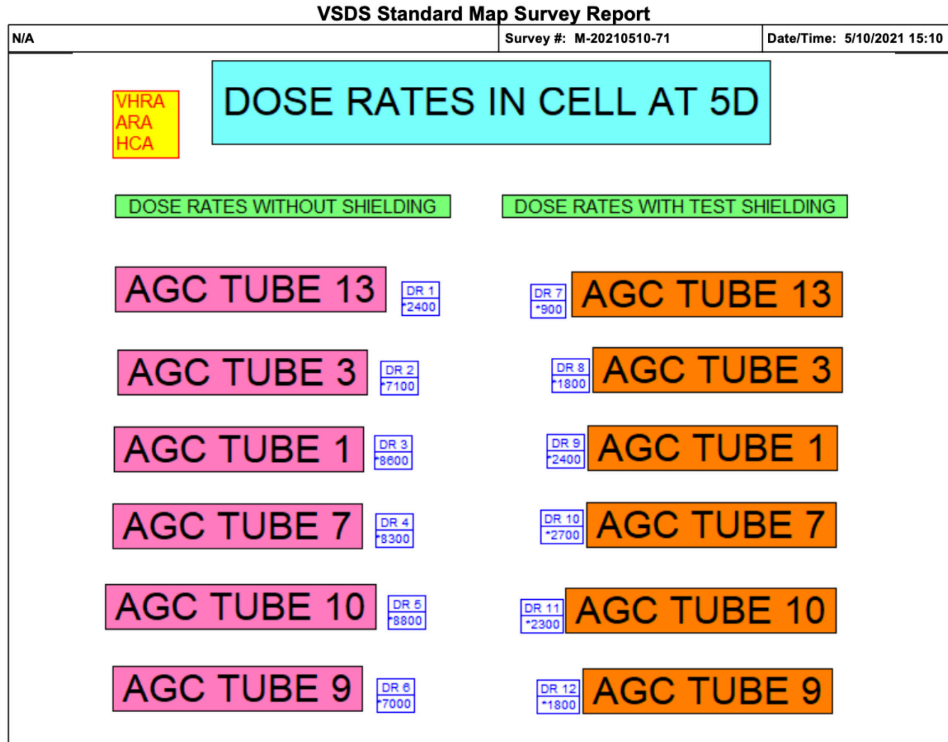


Figure 13. AGC-4 shipping tubes survey with and without shielding. (Dose rates are in millirem per hour, indicated in the blue box with a * indicating a contact reading, nominally 2 cm from the face of the detector. Values are beta+gamma, reported with a 3x correction factor)

After removing all graphite specimens and flux wire spacers, the graphite body sections were reassembled to the extent possible and dimensional measurements were performed, as shown in Table 2. The various sections were placed on the sorting table tray, and the Vernier caliper was used to check each section's length, seen in Figure 14. The sections were measured, however possible based on sector orientation.



Figure 14. Image of the caliper measuring the graphite body.

Table 1. Graphite body physical measurements.

Graphite Body	Dimension (in)
Length	47.537
Upper sections	8.937, 12.955
Lower sections	8.569, 9.215, 7.861
Break (bottom) end to first gas ring slot	8.365

2.2.2 Dose Rate Evaluations

At the time of this report (July 13, 2021), the following efforts have been made:

- Survey of tubes of packaged creep and piggyback samples.
- Decontamination of the tubes to the level that smears indicates no removable contamination.
- Measurement of non-specimen components (shuttle pistons) using the HFEF Main Cell Precision Gamma Scanner (five shuttle pistons in a Lexan shipping tube were non-detectable).
- Measurement of one of the highest activity tubes of creep specimens using the Precision Gamma Scanner indicated the presence of ^{60}Co as seen in Figure 15 below. No explicit quantitation was performed.
- One creep specimen from each of three of the highest activity transfer tubes was removed and packaged to be shipped to the MFC Analytical Laboratory (AL) for gamma spectrometry measurement in a low-background shielded system to measure all detectable gamma emitters and their quantities.
- In addition to the high-activity creep samples, one flux wire (fluence capsule) will also be shipped to the MFC AL for comparison to previous flux wire values (AGC-2) to ascertain whether unexpected flux levels were achieved during irradiation.

- The above-mentioned samples have been transferred to the MFC AL, and the dose rates at the time of transfer were reported as 25 R/hr contact and 500 mR/hr at 30 cm, indicating a bias toward beta emissions.
- Analysis currently proposed for determining the source the unexpected dose rates includes gamma spectrometry as well as laser-induced breakdown spectrometry (LIBS)/time-of-flight mass spectrometry (TOF-MS) to identify and measure isotopes that are exclusive beta emitters such as ^{63}Ni .

Isotope	Channel	Energy	Background	Net Counts	Count Rate			X Position	Z Position	File Name
CO-60	4280.66	1173.79	301	6477	0.386	1.36	1.903	5.44	22	20210603-162311-AGC4_875profile_0001.chn
CO-60	4280.78	1173.82	324	6248	0.372	1.41	1.903	5.44	22.875	20210603-162311-AGC4_875profile_0002.chn
CO-60	4280.69	1173.8	68	302	0.018	7.99	2.036	5.44	23.75	20210603-162311-AGC4_875profile_0003.chn
CO-60	4280.8	1173.83	86	1402	0.083	3	1.878	5.44	24.625	20210603-162311-AGC4_875profile_0004.chn
CO-60	4280.79	1173.82	2099	47176	2.808	0.51	1.895	5.44	25.5	20210603-162311-AGC4_875profile_0005.chn
CO-60	4280.92	1173.86	480	10137	0.603	1.09	1.907	5.44	26.375	20210603-162311-AGC4_875profile_0006.chn
CO-60	4280.93	1173.86	65	705	0.042	4.35	1.799	5.44	27.25	20210603-162311-AGC4_875profile_0007.chn
CO-60	4280.19	1173.66	61	437	0.026	5.94	1.717	5.44	28.125	20210603-162311-AGC4_875profile_0008.chn
CO-60	4280.97	1173.87	58	946	0.056	3.66	1.87	5.44	29	20210603-162311-AGC4_875profile_0009.chn
CO-60	4280.88	1173.85	96	1226	0.073	3.29	2.054	5.44	29.875	20210603-162311-AGC4_875profile_0010.chn
CO-60	4280.87	1173.84	55	208	0.012	9.5	2.074	5.44	30.75	20210603-162311-AGC4_875profile_0011.chn
CS-137	2413.81	662.04	115	71	0.004	28.01	1.718s	5.44	31.625	20210603-162311-AGC4_875profile_0007.chn
MN-54	3045.66	835.26	320	111	0.007	28.7	1.872s	5.44	32.5	20210603-162311-AGC4_875profile_0002.chn
MN-54	3047.37	835.73	2617	395	0.024	23.33	1.793s	5.44	33.375	20210603-162311-AGC4_875profile_0005.chn

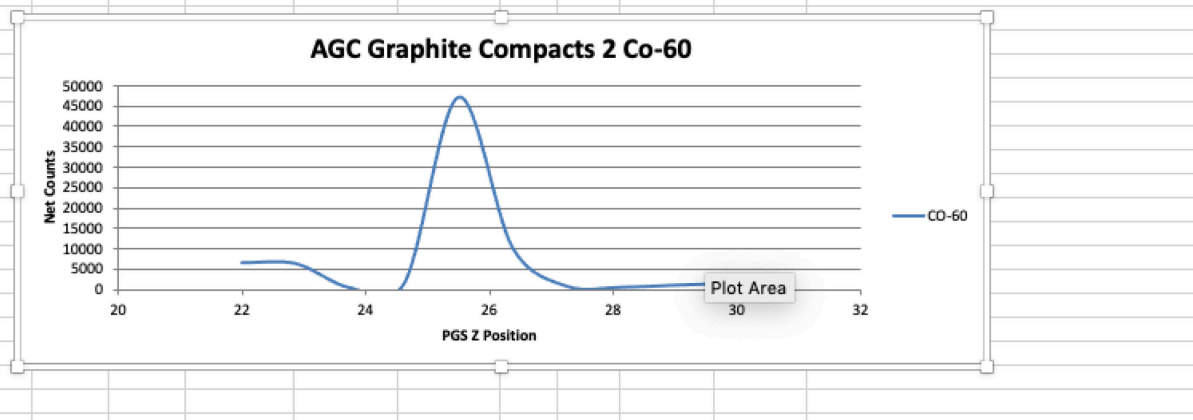


Figure 15. Preliminary results precision gamma scanner creep specimens (Hawkins 2021).

3. CONCLUSIONS FROM AGC-4 CAPSULE DISASSEMBLY ACTIVITIES

The pipe cutter appears to have some slight difference in centerline height compared to the carriage clamps. This leads to a challenge in getting the collet completely tight to prevent the test train from rotating when the cutter blade pulls up a curl that is greater than the friction the collet can hold. This was a particular problem at the very end of the cut above the cap joint. One blade had apparently broken off its edge, but it was possible to complete the cut after manually repositioning the other blade. To minimize the problem of raising a large curl, the cutter was operated in the mode where the cutter advance lever was engaged for two rotations of the cutter drive, then disengaged for one rotation, allowing the cutters to clear the curls and break any large pieces prior to continuing the cut. The pipe cutter will be utilized for future AGC capsule disassembly activities. It may be desirable to have a reversible drive for the cutter to ease the process of disengaging the cutters following the cut, as well as to allow the cutter to back up from a point where the blade has caught.

The graphite body length caliper appears to work well and needs no modification. The biggest challenge in the length determination is identification of specific datums from which to make

measurements. The top cut is not a precisely controlled process, so measurement must be made from one of the separation joints, the most definitive of which are the slots that are machined to hold gas sector control ring. The bottom and middle section separations occurred due to mechanical stresses when milling, meaning that more separate parts resulted from disassembly than were originally manufactured, hence the multiple length values in the table above.

The anomalous dose rates have caused several lines of speculation to be considered, mostly having to do with identifying a mechanism by which an activation product such as ^{60}Co could have entered the specimens. At such time that the data are available, it may be possible to transfer some or all the creep and piggyback samples to CCL for further post-irradiation examination. Operations in CCL may require procedural or engineering modifications to minimize personnel dose. An early presumption that the samples had become contaminated with fission products from the HFEF Main Cell environment cannot be supported, in that gamma spectrometry results from survey and separation of high-dose samples do not show appreciable fission product isotopes. The dose rate limit in CCL is set by the Radiological Work Permit as 100 mR/hr.

3.1 Handling and Survey of High-Dose Rate Samples

After determining that all of the individual sample transfer tubes had dose rates greater than the nominal upper limit of 100 mR/hr at contact, individual samples were removed from selected tubes to determine whether all samples were high activity. The selected samples were taken from the highest dose rate tubes, and found to be in the 1-5 mR/hr range. Based on that knowledge, a decision was made to move the samples from the HFEF decon cell to the MFC Analytical Laboratory Special Projects Glovebox (SPGB) for survey in a low-background location. A glovebox operation was chosen due to the possibility that the samples had somehow been grossly contaminated in the HFEF Main Cell. The relatively small number of high activity samples and low contamination levels observed during surveys in the Special Projects Glovebox support the conclusion that Main Cell contamination was not a significant source of the high activity on the AGC-4 specimens. Proximity to the MFC-752 Hot Cells allowed for high-activity samples to be transferred into a location where anomalous dose contribution could be measured by gamma ray spectrometry. The west section of the glovebox was not in use at the time, and thus was selected as a flexible low-background workspace.

Preparation for that process was made by doing thorough decontamination of the glovebox to minimize the potential for contaminating otherwise clean samples. Lead brick shielding was installed in the glovebox following engineering evaluation of the load capacity of the glovebox floor. A miniature digital microscope was inserted into the box to allow clear identification of sample numbers without personnel moving the sample unnecessarily close to the window. A medium range ion chamber was set up to provide a means to identify localized high activity within the sample transfer tubes. This detector was mounted in a heavy steel shield to minimize background from other material within the glovebox or in the sample tubes. Samples were initially surveyed with the shielded ion chamber and then checked for transfer to a hood using a standard hand-held Eberline RO-20 ion chamber through the glovebox glove. The shield is shown in Figure 16 and the general arrangement is shown in Figure 17.

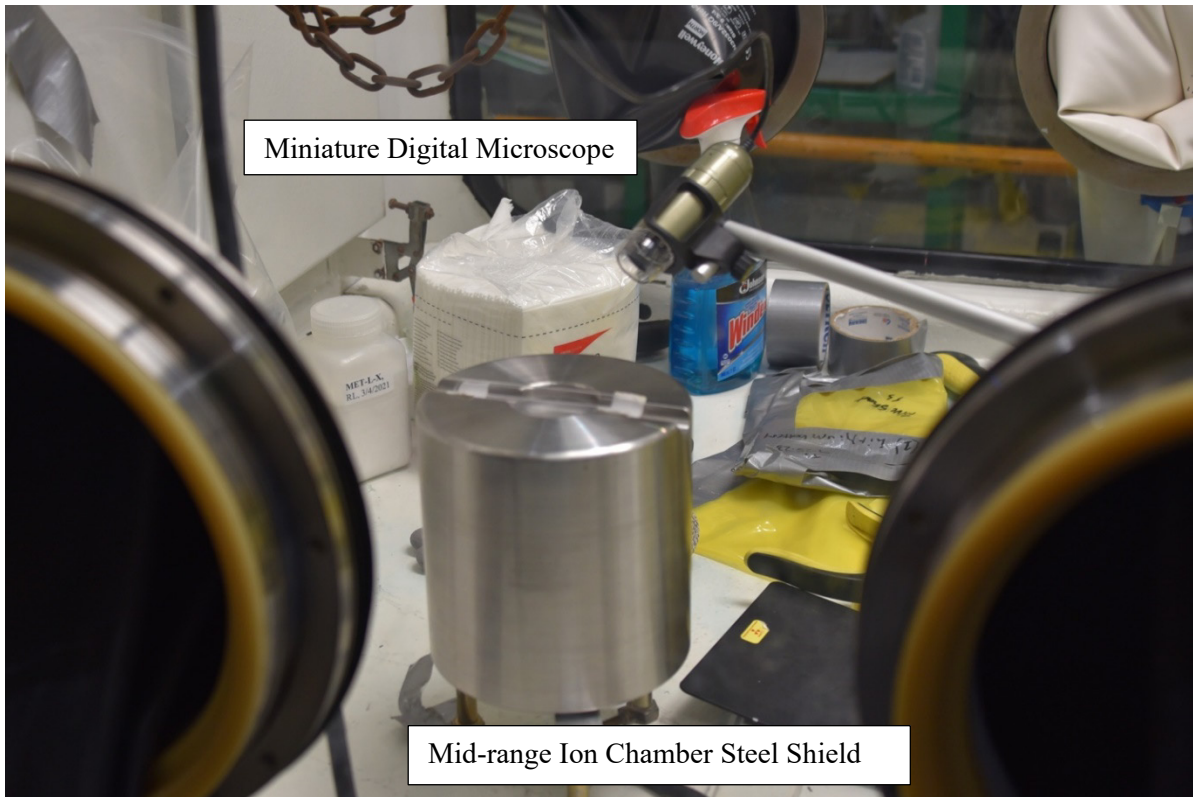


Figure 16. Steel detector shield with microscope.



Figure 17. Survey equipment in glovebox.

The survey and decontamination was performed in stages. The first step was to retrieve a sample tube from the shielded drum and transfer it into the Special Projects Glovebox by inserting it into a sleeve and “punching” it in through a glove port. Once inside, it was surveyed and the individual samples were separated into those having dose rates less than and those greater than 100 mR/hr. Samples less than 100 mR/hr were transferred from the SPGB in the A-wing to either of two hoods in the B-wing of MFC-752. Hood operations are less difficult for those doing work because movement is easier when not constrained within a fixed glove port.

Due to staffing limitations at the AL, only approximately one-third of the sample tubes were able to be surveyed, samples segregated, and decontaminated to the nominal levels that are necessary for work on the benchtop in the CCL. AL personnel made substantial progress despite only working overtime on several weekends, but were not available full-time. It was determined that personnel and equipment for completing survey of the remaining sample tubes were available at the Electron Microscopy Laboratory (EML), MFC-774. The shielded transfer drum was transferred to EML and after some familiarization, the survey and decontamination process was completed. The massive lid for the shielded drum is being lifted in Figure 18. Figure 19 shows the manual survey and decon actions in process.



Figure 18 Opening the Shielded Drum at EML



Figure 19 Survey and Decon in EML Hood

Approximately 90% of the samples were determined to be within the range of 1 to 10 mR/hr beta-gamma on contact, and only negligible alpha contamination was detected. The high-activity samples ranged from 100 mR/hr to a maximum corrected value of 8.8 R/hr beta-gamma at contact (Specimen DW5503). Gamma spectrometry of select examples of the high-activity samples indicates that the dominant gamma ray emitting isotope was cobalt-60. Secondary analysis was performed to determine if other contaminants were present. Laser-induced breakdown spectrometry/time-of-flight mass spectrometry measurements indicated the presence of copper as well as nickel and chromium. Conventional mass spectrometry was used to measure metals in solutions that were derived from dissolving the ash residue from oxidizing the samples in an air environment furnace at 750°C. Those analyses also indicated the potential presence of iron and nickel. Isobars at mass 55 and 63 limit the possibility of making a definitive measurement. That sample will be reanalyzed using optical emission spectrometry to do an elemental rather than mass measurement.

All samples surveyed and decontaminated at MFC that met the low activity standard have been packaged for transportation to IRC CCL. Approximately 60% of the low-activity creep specimens were also measured for dimensional changes using a non-contact optical micrometer.

The sample transfer tubes that had activity levels too high for glovebox handling were transferred to the MFC-752 AL hot cells. In the hot cell, separation and survey handling was done with a reduced number of personnel, since radiological control technicians did not need to do the primary survey. In the hot cells individual high-dose rate samples were separated from those low enough to be transferred to the IRC. The in-cell primary survey was performed using a gamma ray spectrometer gross gamma count and a correlation factor to predict gamma dose rate. This required only one person to separate and characterize high-activity samples. Previous efforts were done in a glovebox and hood, and required a minimum of three people to cover radiological control and sample manipulation. High-activity samples from that effort were measured by gamma spectrometry and found to contain unexpected levels of the steel activation

product, cobalt-60. Relatively minimal amounts of contamination that can be linked to the disassembly process in the HFEF hot cell have been found during all activity measurements.

Prior to shipment to AL, efforts to identify the source of high activity using the HFEF Precision Gamma Scanner (PGS) provided inconsistent results. The graphite shuttle pistons that were located at the very center of the experiment, separating stressed from unstressed specimens, were measured using the PGS, and were essentially undetectable over cell background. It was expected that these components would be high activity to the same degree as the highest found in the system. The tube containing the shuttle pistons was transferred to MFC-752 with the highest activity tubes, and when those tubes were transferred to the hot cells, the shuttle piston tube was surveyed in a low-radiation background and found to be on the order of 4 to 5 mR/hr on contact, which explains the inability of the HFEF PGS to detect the pistons above cell background. The samples that have been evaluated to date have not provided a pattern that would link the high-dose samples with a particular material transfer or temperature transient. Sample DA4809 exceeded 500 mR/hr was measured using the AL Hot Cell 4 gamma spectrometer and the dominant isotope was Co-60 by two orders of magnitude. (See Figure A-1). Efforts to remove that activity were done by wiping the exterior surface with ammonia solution and by leaching with 8 molar hydrochloric acid. These decontamination actions did not have a measurable effect. This suggests that the high activity within specific specimens is not superficial contamination that can be readily removed. However, low-activity samples with surface contamination identified during the survey and segregation process in the AL and EML operations were successfully decontaminated using conventional surface wiping with cellulose towels dampened with ammonia glass cleaner. Those efforts were consistently effective. An excerpt from a listing of survey data is shown in Table A-1.

At the date of this report, seventy-two high-activity creep and piggyback specimens were either retained at the AL or transferred there following survey and decontamination at the EML. Thirty-five samples were separated at AL and thirty-seven were found during work at EML. A partial listing of those samples is shown in Appendix Table A-2. This listing is noted as interim, because several sample IDs were illegible and data from the last tube of samples has not been reported. It is hoped that better identification of illegible sample IDs can be achieved using the AL Hot Cell 5 microscope.

A non-contact optical micrometer was acquired and fixtures for doing length and diameter measurements of creep samples were developed. This method is being used at EML to catalog dimensions of the creep specimens during the survey and decontamination process. The fixtures allow the sample to be rotated to measure various diameters and moved laterally to evaluate concentricity. Images of the equipment and fixtures are shown in Figure 18 and Figure 19. The micrometer projects a light beam (seen as a green line visible on the aluminum standard in Figure 19).



Figure 20. Keyence LS7070M optical micrometer.

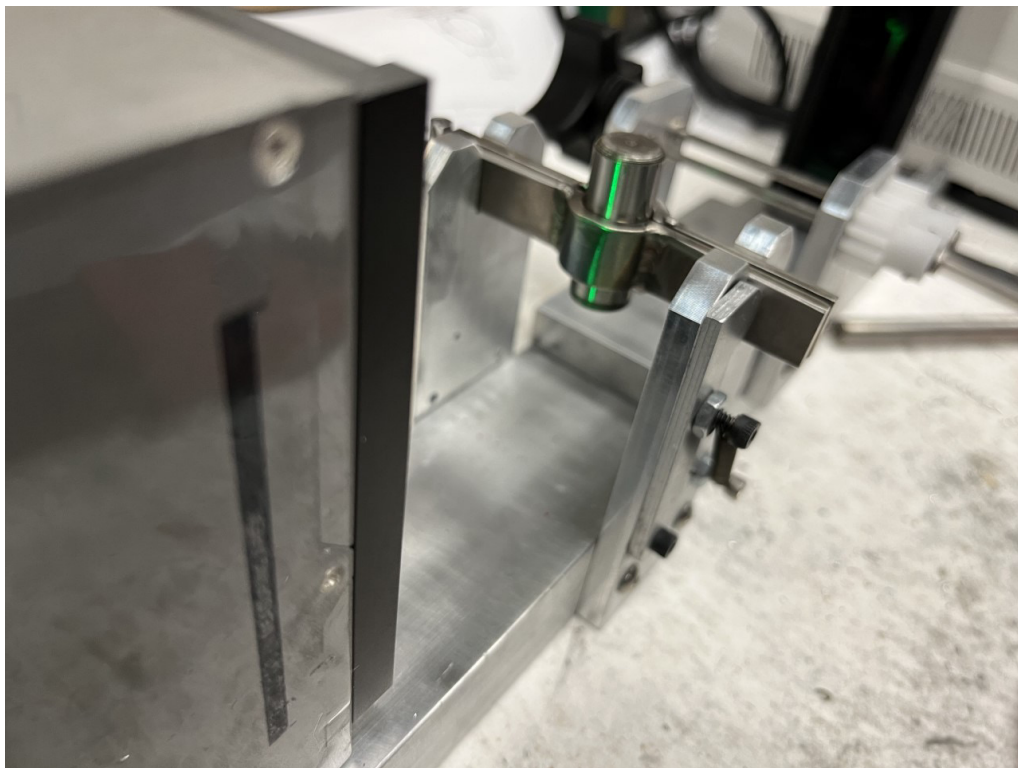


Figure 21. Visible projected beam from optical micrometer with aluminum standard.

3.2 Visual Inspection of AGC-4 Specimens

As shown in Figure 20, full-size creep specimen AP4804 shows no significant identifiable anomalies, either in terms of coloration or mechanical damage. This image was produced by the miniature digital microscope during the sample identification process. To ease the task of identifying samples, a polyethylene pedestal was fabricated to allow the technician to position the sample in the focus range of the microscope and rotate the hexagonal portion to read the sample number and note anomalies (see Figure 21).



Figure 22. Visual inspection example using miniature digital microscope in glovebox.

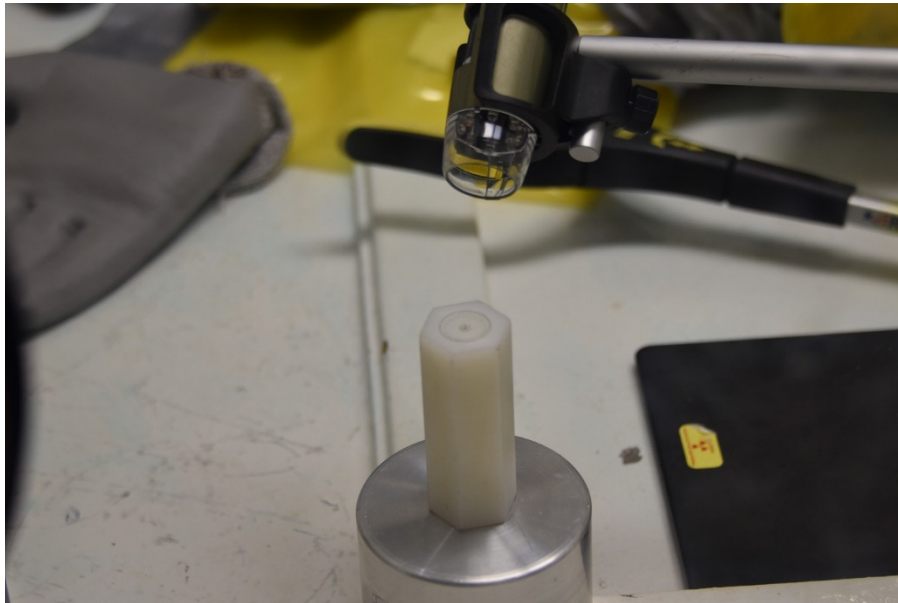


Figure 23. Rotary pedestal for specimen inspection.

3.3 Characterization of High-Dose Rate Samples

Due to the time-consuming and resource-limited process of separating, decontaminating, and packaging the samples, a limited amount of the high-dose samples were characterized beyond the determination of external dose rate. Those that have been separated will be measured by non-destructive gamma spectrometry, time-of-flight/laser-induced breakdown spectrometry (TOF/LIBS) or X-ray fluorescence (XRF), followed by oxidation and either mass spectrometry or optical emission spectrometry of the leach solution. XRF provides only proportional elemental indications, and in this case the measurement indicated a relatively high fraction of the metals present was manganese, followed by iron and copper. This measurement cannot be converted to a parts-per-million value because it was not compared to a standard sample of the same composition with a known metals content. As a surface measurement, it also cannot be used to determine metals content within the bulk of the sample. Carbon is not detected in this measurement. CAN-114 was 400 mR/hr on contact when surveyed, and was selected for analysis using TOF/LIBS and XRF. The results of the XRF measurement are shown in Figure 22.

In TOF/LIBS, a minute portion of the surface is ablated using a laser, and the immediate spectrum produced by electron relaxation provides an elemental signature, and the physical sample is transported downstream to a mass spectrum detector that identifies mass by the delay between the initial volatilization by the laser and the time it reaches the detector. The system produces a graphical image of the location that is scanned by the laser, and an image of the areas of relatively high concentrations of metals is produced. The image in Figure 23 shows the sample and the red box is the area scanned. The area shown in the left image in Figure 24 shows a location with relatively higher metal concentration as a lighter yellow oblong artifact in the upper-mid (52.6) section of the scan. This correlates to a localized area with higher iron.

```
Sample : Line Side
Operator: Nick/Matt
Comment : Sample #1
Group   : AGC4 Graphite
Date    : 2022-12-20 15:47:38
```

```
S-K           ArKa      2.96    0.7438    QF
              ArKb      3.20    0.0818
              CaKa      3.68    0.0351
```

 Quantitative Result

Analyte	Result	[3-sigma]	Proc.-Calc.	Line	Int. (cps/uA)
Mn	28.763 %	[0.538]	Quan-FP	MnKa	13.1681
Fe	27.642 %	[0.427]	Quan-FP	FeKa	18.3869
Cu	21.918 %	[1.652]	Quan-FP	CuKa	19.1169
Si	10.858 %	[2.531]	Quan-FP	SiKa	0.0444
S	8.131 %	[0.860]	Quan-FP	S Ka	0.2522
Ca	2.688 %	[0.392]	Quan-FP	CaKa	0.2443

Figure 24. X-Ray fluorescence detection of elemental contamination in AGC-4 sample.

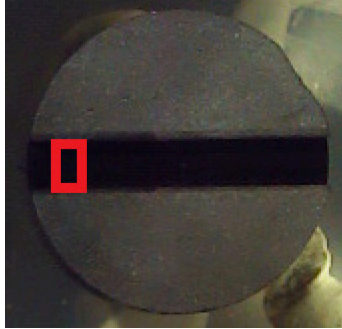


Figure 25. Image of CAN-114 area scanned by TOF/LIBS detector system.

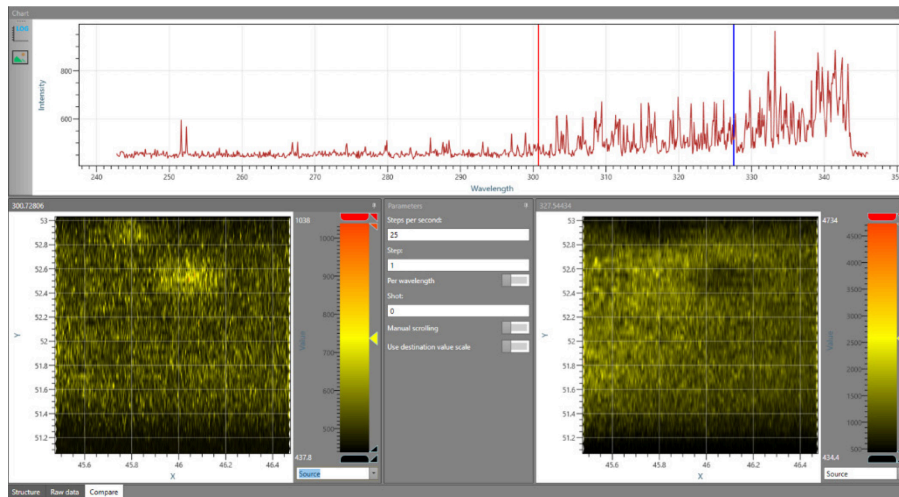


Figure 26. TOF/LIBS spectral and visual display of indicated CAN-114 specimen.

Gamma spectrometry of the high-activity samples confirms that the selected samples have higher-than-expected concentrations of cobalt-60. Sample DA4809 was measured as having a dose rate of 900 mR/hr corrected beta+gamma, and transferred to the hot cell for further characterization. The results from gamma spectrometry and mass spectrometric analyses is reported in Figure A-1.

The data shown in Table 3 come from measurements done with the samples in AL Hot Cell 4, which uses a gamma spectrometer that detects the sample via a through-wall penetration. There is a low-level background of Cs-134/137 and Eu-154/155 fission product activity in the cell that is detected by the spectrometer. The detection of these isotopes is orders of magnitude lower than the Co-60. This confirms that the contamination from the HFEF hot cell during disassembly is not likely to be the cause of the high activity in selected samples. Contamination in HFEF is dominated by fission product, not activation product isotopes due to Main Cell fuel dissolution and process activities. The fact that the high-dose cobalt activity is not reduced by manual wiping nor by leaching in acid suggests that the contamination is integral, not superficial. With a specific activity of 1100 Ci/g, a value of 4.4 millicuries (4.39E3 microcuries) of Co-60 as seen in sample DW570x would produce a point source dose rate of 14 R/hr at 2 cm (effective contact). This is generally consistent with the highest dose rates seen.

Table 3. Preliminary gamma spectrometry data; high-dose AGC-4 specimens.

Gamma Spectrometry - Preliminary results								
	DW570x		BP4602		DW5001		BL4002	
	Result ($\mu\text{Ci}/\text{sample}$)	Error	Result ($\mu\text{Ci}/\text{sample}$)	Error	Result ($\mu\text{Ci}/\text{sample}$)	Error	Result ($\mu\text{Ci}/\text{sample}$)	Error
Co-60	4.39E+03	$\pm 7\%$	1.58E+02	$\pm 7\%$	3.19E+03	$\pm 7\%$	1.39E+02	$\pm 7\%$
Cs-134	Not identified		1.37E+00	$\pm 7\%$	Not identified		1.57E+00	$\pm 7\%$
Eu-154	5.10E+00	$\pm 20\%$	Not identified		6.90E+00	$\pm 10\%$	Not identified	
Eu-155	2.32E+00	$\pm 22\%$	Not identified		3.57E+00	$\pm 13\%$	Not identified	
Mn-54	4.10E+00	$\pm 22\%$	4.20E-01	$\pm 32\%$	3.50E+00	$\pm 20\%$	Not identified	

4. INTERIM CONCLUSIONS

It is clear from the survey, separation and decontamination efforts performed following removal of the samples from HFEF that although numerous samples have higher activity than those resulting from AGC-1, 2, and 3, these are not the majority of the AGC-4 experiment's 440 specimens. Evaluation of the locations of the high-activity samples has not led to a determination of a consistent explanation of a cause of the metal transfer, such as the proximity of thermocouples or other metal components of the experiment. Cobalt-60 has been consistently detected in the high-activity samples. The samples that have been measured by other chemical and spectroscopic techniques also show unexpected and unexplained content of other metals such as manganese, copper, and iron. A full evaluation that maps the high-dose samples relative to their location in the experiment will be completed when all of those samples have been identified and cataloged. At the time of this report, not all high-activity samples have been measured with gamma spectrometry, and not all samples have been transferred to the IRC CCL for full characterization.

5. REFERENCES

Davenport, M. E., "DP-AGC-4, Data Package for AGC-4," Advanced Reactor Technologies (ART) August 2019.

Davenport, M. E., "As-Run Physics Analysis for the AGC-4 Experiment Irradiated in the ATR." ECAR-5345. Idaho National Laboratory. January 2021.

Hawkins, K. A. Email transmission of PGS data. June 22, 2021.

INL. (2012) "Advanced Graphite Capsule, Capsule Facility Assemblies." Drawing 630430. Idaho National Laboratory. July 09, 2012.

INL. (2014) "ATR Advanced Graphite Capsule (AGC-4) Test Train Facility Assembly." Drawing 604554. Idaho National Laboratory. July 08, 2014.

Swank, W. D. (2012) "Graphite Specimen Preirradiation Characterization Plan." PLN-4239. Idaho National Laboratory. August 2012.

Windes, W.E., T. Burchell, and R. Bratton. (2010) "Graphite Technology Development Plan," PLN-2497. Rev. 1. Idaho National Laboratory. October 2010.

Appendix A

INL - Materials and Fuels Complex Analytical Laboratory

Final Report				
AL Log #:	110958	19-Apr-23 9:14 am		
LabWare Number:	69797			
Login Name:	AGC-4 Sample DA4809			
Requester:	Winston, Philip L.	Charge #:	103767344	
Sampling Location:	AL	Date Received:	11/21/2022 10:02:46AM	
Approved By:	Luiza Gimeres Rodrigues Albuquerque	Date Approved:	4/19/2023 9:14:34AM	
Sample ID:	AGC4 DA4809	Sampling Date:	11/17/2022 9:56:50AM	
Description:	Nuclear Grade Graphite Ash Leached			
Analytical Method	Analyte	Result	Units	Error @ 2 Sigma
GAMMA_SPEC				
	Co-60	1.50E+1	µCi/g	±3%
	Cs-137	8.5E-3	µCi/g	±27%
	Mn-54	4.23E-2	µCi/g	±4%
	Eu-155	1.1E-2	µCi/g	±36%
Comments:				
LIQUID_SCINTILLATION				
	Gross Alpha	5.29E+06	DPM/mL	±1%
	Gross Beta	1.40E+07	DPM/mL	±1%
Comments:				
Q_ICP_MS	Results	Please see comments	-	
Comments: The isotopes requested (Fe-55 and Ni-63) are prone to isobaric mass interferences from Mn-55 and Cu-63. Thus, the results are reported as mass-to-charge ratios, as these isotopes cannot be specifically determined by Q-ICP-MS. Below are reported all mass-to-charge ratios measured.				
	M/Z-55	0.0256 ug/sample ± 10%		
	M/Z-58	2.48 ug/sample ± 5%		
	M/Z-60	2.57 ug/sample ± 5%		
	M/Z-62	2.30 ug/sample ± 5%		
	M/Z-63	0.139 ug/sample ± 5%		
	M/Z-65	0.0608 ug/sample ± 5%		

Figure A-1 Analysis of Oxidized Sample DA4809

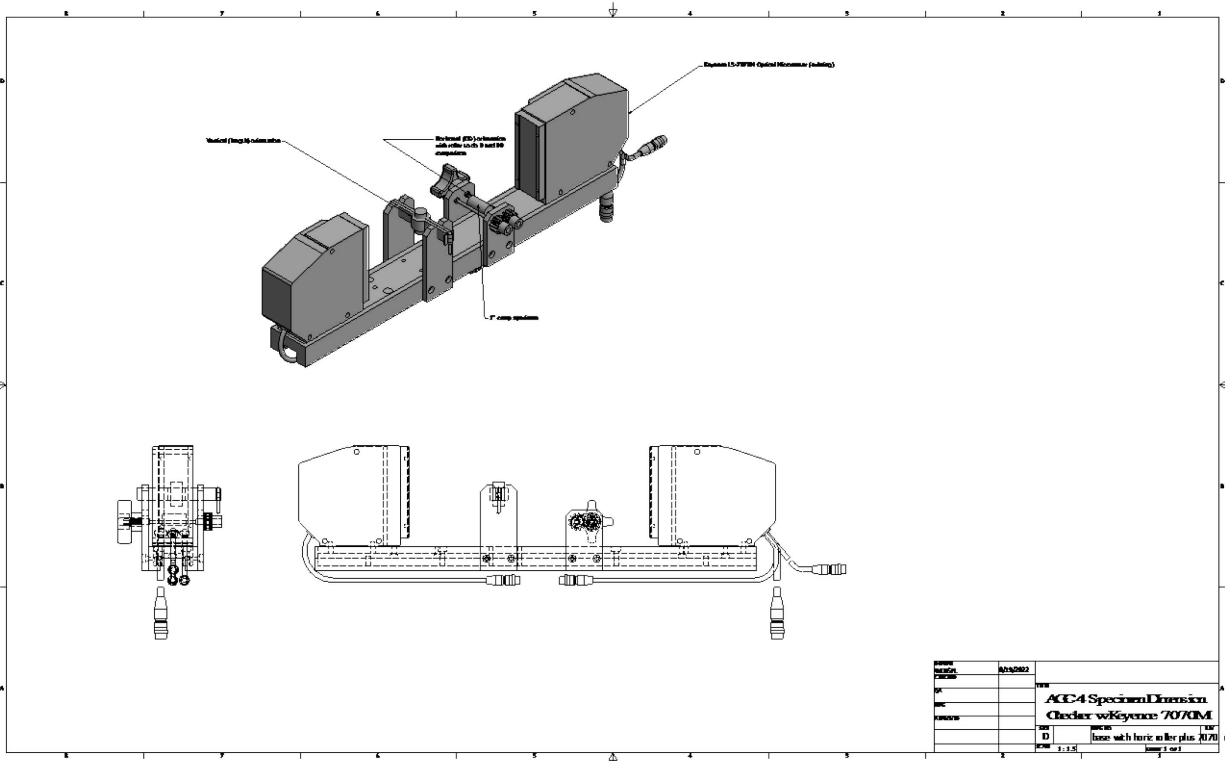


Figure A-2. General configuration sketch for optical micrometer.

Table A-1. Example survey data for select samples handled in AL hood. (Dose rates are in millirem per hour, OW is Open Window, nominal total beta+gamma, CW is Closed Window, nominally gamma only)

Sample Number	Dose Rate IN B 119 Hood
BP3909	OW 18 CW 12
AP5801	OW 10 CW 6
AP5804	OW 18 CW 11
CAN106	OW 3 CW 1.2
TW4302	OW 9 CW 8
TW4918	OW 9 CW 6
CAN139	OW 7 CW 7
EA4801	OW9 CW 7
EA6310	OW 4.5 CW 3.8
AW4903	OW 35 CW 22

Table A-2. Interim Listing of Samples in Excess of 100 mR/hr (* indicates partially or completely illegible, or uncertain ID)

Sample Number	Material	Sample Number	Material	Sample Number	Material	Sample Number
AP5804	NBG-17A	DW4902	PCEA-W	DW5404	PCEA-W	Z01
BP3904	NBG-18A	DW4903	PCEA-W	DW5501	PCEA-W	Z03
BP4612*	NBG-18A	DW4904	PCEA-W	DW5503	PCEA-W	Z04
BW4401	NBG-18	DW5001	PCEA-W	DW5601	PCEA-W	Z06
CAN113	HOPG	DW5102	PCEA-W	DW5603	PCEA-W	Z07
CAN115	HOPG	DW5103	PCEA-W	DW5604	PCEA-W	Z09
DA4210*	IG-110	DW5104	PCEA-W	DW570x*	PCEA-W	Z11
DA4113*	IG-110	DW5201	PCEA-W	DW5804*	PCEA-W	Z12
DA4806	PCEA-A	DW5202	PCEA-W	DW6203	PCEA-PB	Z14
DA4807	PCEA-A	DW5302	PCEA-W	DW6204	PCEA-W	Z18
DW4209*	PCEA-W	DW5304	PCEA-W	DW8203*	PCEA-W	
		DW5401	PCEA-W	*N/A couldn't read		*4804
		DW5403	PCEA-W	*N/A couldn't read		*4812

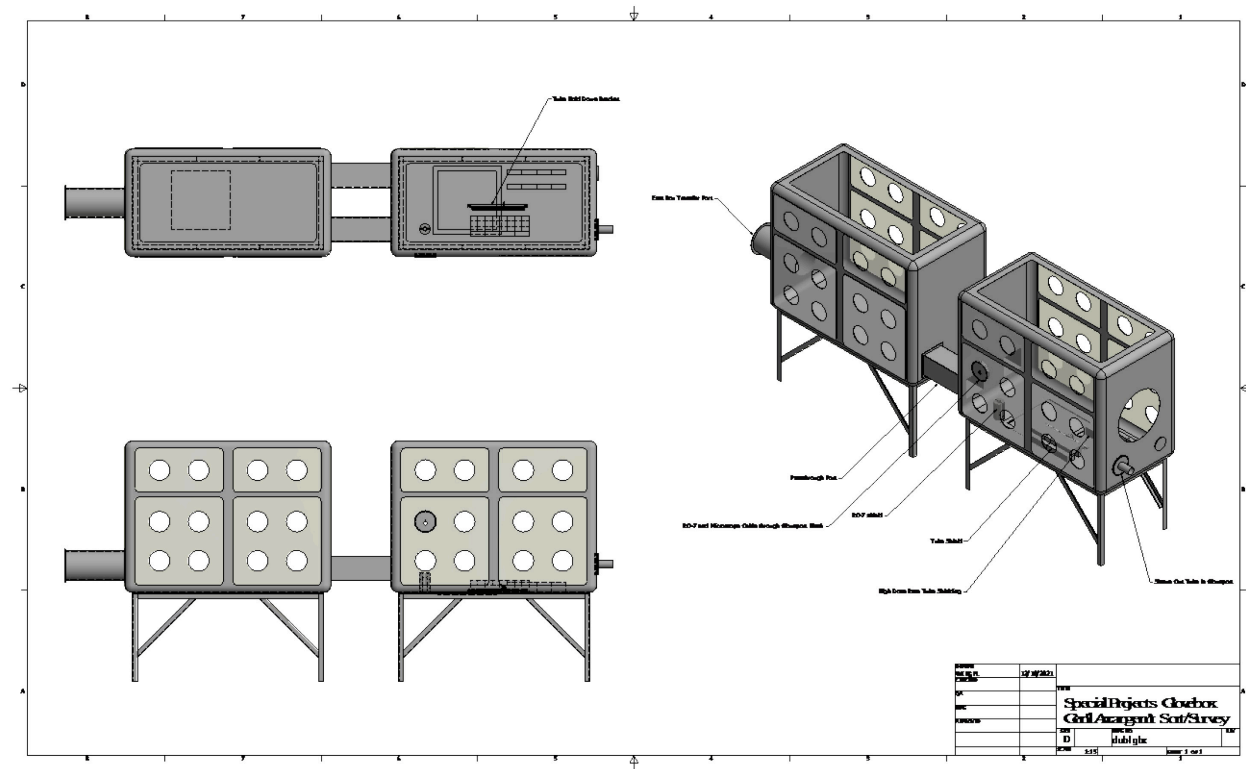


Figure A-3. MFC AL special projects glovebox general layout for sample survey/decon.